Journal of Hazardous Materials 346 (2018) 27–35

Contents lists available at ScienceDirect

Journal of Hazardous Materials

journal homepage: www.elsevier.com/locate/jhazmat

Evaluation of carbon nanotube based copper nanoparticle composite for the efficient detection of agroviruses

Muhammad Ali Tahir[a,c,d], Sadia Z. Bajwa[a], Shahid Mansoor[a], Rob W. Briddon[a], Waheed S. Khan[a], Brian E. Scheffler[b], Imran Amin[a,*]

[a] National Institute for Biotechnology and Genetic Engineering (NIBGE), Faisalabad, Pakistan
[b] USDA ARS, Genomics and Bioinformatics Research Unit, P.O. Box No. 36, Stoneville, MS 38776, USA
[c] Pakistan Institute of Engineering and Applied Sciences (PIEAS), Nilore, Islamabad, Pakistan
[d] Department of Environmental Science and Engineering, Fudan University, Shanghai, 200433, P.R. China

HIGHLIGHTS

- Carbon nanotubes based copper nanoparticles composite can be used to develop biosensor for the detection of a begomovirus (CLCuKoV-Bur).
- The morphology of composite consists of copper nanoparticles (20–100 nm) anchored along the whole lengths of tubes.
- The developed sensor exhibits excellent ability to detect CLCuKoV-Bur selectively up to 0.01 ng μL^{-1} DNA concentration.

GRAPHICAL ABSTRACT

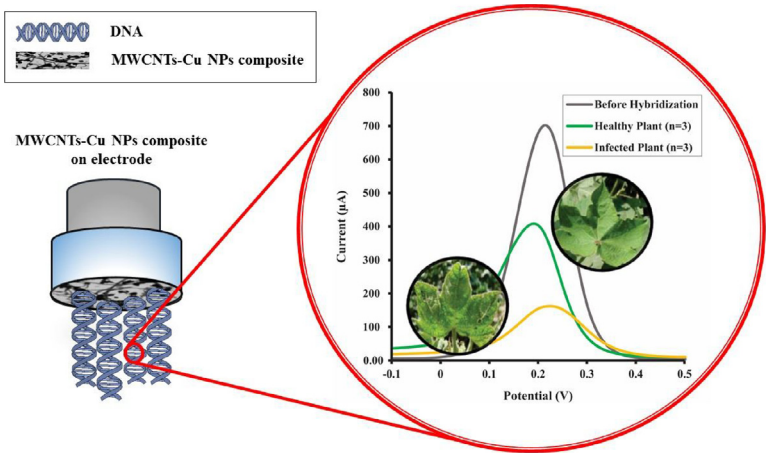

ARTICLE INFO

Article history:
Received 26 July 2017
Received in revised form
30 November 2017
Accepted 3 December 2017
Available online 5 December 2017

Keywords:
Carbon nanotube composite
Copper nanoparticles
Electrochemical detection
DNA biosensor
Agroviruses

ABSTRACT

We report a biosensor that combines the construction of a three-dimensional nanocomposite with electrochemical methods for the detection of viruses in plants. This is the first report, where carbon nanotubes are used as a conductive frame to anchor highly electrolytic agglomerates of copper nanoparticles to detect agroviruses. Morphological analysis of nanocomposite revealed the presence of carbon nanotubes having a diameter of 50–100 nm with copper nanoparticles of 20–100 nm, attached in the form of bunches. This material was applied to assess the infection caused by geminiviruses which are a major threat to the cotton plants in Asian and African countries. The hybridization events were studied by monitoring differential pulse voltammetry signals using methylene blue as a redox indicator. In the presence of target DNA, sensor signals decreased from 7×10^{-4} to 1×10^{-4} Ampere. The probe exhibited 97.14% selectivity and the detection limit was found to be 0.01 ng μL^{-1}. The developed biosensor is stable for at least four weeks, losing only 4.3% of the initial signal value. This sensor was able to detect the presence of viruses in sap extracted from cotton leaves, thus providing a promising platform to detect a range of other crops-infecting viruses.

* Corresponding author at: Department of Environmental Science and Engineering, Fudan University, Shanghai, 200433, P.R. China.
E-mail address: imranamin1@yahoo.com (I. Amin).

https://doi.org/10.1016/j.jhazmat.2017.12.007
0304-3894/

1. Introduction

The interaction between nanomaterials and bio surfaces can be harnessed for the development of efficient interfaces for optical, electrical, mechanical, and electrochemical detection of various biologically important molecules and cells [1]. In particular, cost-efficient, but selective, nano/bio interface based DNA sensors have attracted much attention as several diseases can be identified by the recognition of unique DNA sequences of a particular pathogen [2]. The basic phenomenon in most types of DNA detection technology is based on the hybridization between a specific DNA probe sequence and its target complementary strand. Various techniques have been developed for DNA identification and among them, the most commonly used technique is polymerase chain reaction (PCR), among other traditional methods like gel electrophoresis or membrane blots [3–5]. However, these methods are slow and laborious for routine analysis and especially for the timely and rapid detection of specific DNA targets. Therefore, there is a dire need to develop a detection method that is simple, low cost as well as accurate and sensitive. To achieve this goal, nanotechnology based interfaces could be one of the efficient options.

Advanced nano-biosensors are versatile tools to develop diagnostic systems for a variety of analytes [6–8]. For the detection of specific DNA sequence or mutated genes associated with infection or disease, DNA biosensors are popular choices because base pairing interactions between complementary sequences are highly specific and faster. The performance and sensitivity of electrochemical biosensor can be improved further by incorporation of functionally important nanomaterials to develop interfaces *e.g* graphene oxide based biosensor based on linkage of graphene oxide sheets with iridium single-stranded DNA (ssDNA) for the detection of target ssDNA [9]. An electrochemical biosensor based on DNA polymerase and HRP-SiO_2 nanoparticles (NPs) has been fabricated for the detection of point mutation in the K-ras gene [10]. Among nanomaterials, carbon nanotubes (CNTs) have attracted greater attention of the scientific community. Their small dimensions, strength and the remarkable physical and chemical properties make them a model candidate for a whole range of promising applications [11]. Here, the increased surface area of CNTs can additionally be used for immobilization of large amounts of a bio probe especially for detection purpose [12]. CNTs cannot be directly employed for DNA detection and other biological reactions because the surfaces of CNTs are chemically inert. However, these can be modified or coated with functional materials for efficient detection [13].

Timely identification of a pathogen can be critical in controlling a disease outbreak in an agricultural production system [14]. Cotton is an important renewable natural fiber, but its production is adversely affected by cotton leaf curl disease (CLCuD) complex, which is basically the group of viruses that belongs to genus *Begomovirus* of the family *Geminiviridae* [15,16]. This disease is spreading fast and has become a threat to the production of cotton in several countries of Asia, South East Asia, and Africa [17].

A large variety of metal nanoparticle-based techniques has been developed for DNA detection since last decade. These techniques received popularity as nanomaterials offer miniaturization and cost-efficient detection along with high sensitivity and specificity. Their unusual optical and electrical properties, their small label size, bioconjugation chemistry make them an exceptional tool for DNA detection [18,19]. These astounding properties of nanomaterials can be assimilated with the electrochemical transducer to construct efficient and sensitive DNA biosensors.

To the best of our knowledge, the present study is the first report describing a functional interface of multi-walled carbon nanotubes copper nanoparticles (MWCNTs-Cu NPs) composite to assess the infection caused by an agriculture related pathogen. For enhanced performance of interfaces, electrical features of metal nanoparticles are combined with high conductivity of MWCNTs. These nanostructures are used to electrostatically bind a probe, specific to virus strain, and the complementary virus DNA. This interface served as a recognition layer of malicious DNA, while greatly amplifying the DNA sensor response due to the synergistic effects of MWCNTs and Cu NPs. To exploit DNA assisted charge transport chemistry upon exposure to complementary DNA, hybridization sequences are monitored as sensor responses by recording electrochemical signals. Further, in the same study, we demonstrate how this DNA-mediated charge transport at the nano-bio interface can be implemented to produce a sensitive assay for the detection of infection in cotton plants.

2. Experimental

2.1. Reagents and materials

All chemicals were purchased either from Merck, Sigma-Aldrich or mentioned otherwise. All the solutions were prepared with ultrapure water from Barnstead™ Smart2Pure™ (Thermo Scientific).

The oligonucleotide sequences used in this study are as follows:

Probe DNA: *Cotton leaf curl Khokran virus*-Burewala strain (CLCuKoV-Bur) clone (acc. no. AM774294)

Complementary Target DNA: CLCuKoV-Bur clone (acc. no. AM774294)

Non-complementary DNA: GroEl gene (acc. no. AF130421). Further specific details of amplification can be found in the supplementary information (SI; sections 1.1 and 1.2).

2.2. Instruments

In this work, Potentiostat/Galvanostat Autolab PGSTAT-12 (Metrohm Autolab B. V.), glass vessel (6.1415.210 Metrohm USA Inc.), Zetasizer Nano ZS (Malvern), thermal cycler C1000 Touch™ (BIO-RAD, USA), NanoDrop™ 1000 spectrophotometer (Thermo Scientific, Wilmington, USA) and Fourier transform infrared spectrometer (FT-IR) model ALPHA FT-IR (Bruker Corporation) were employed. For morphological characterization of MWCNTs-Cu NPs composite and MWCNTs a field emission scanning electron microscope (FESEM) model JSM-7500F (JEOL, Japan) equipped with a transmission electron detector was used. Root mean square (RMS) was calculated using an atomic force microscope (AFM) model SHIMADZU WET-SPM 9600 (Kyoto, Japan).

2.3. Preparation of MWCNTs-Cu NPs composite

First, MWCNTs were functionalized and to do this, MWCNTs (0.03 gm) were dispersed in 5 mL methanol solution of PEI (1% v/v). The mixture was sonicated for 2 h and then maintained at room temperature for another 2 h. Next, these MWCNTs wrapped with PEI, were dispersed in 40 mL methanol until a stable colloid was formed. After colloid formation, $CuCl_2$ solution (0.1 M in methanol; 10 mL) was added to the mixture and stirred for 30 min at room temperature. Then $NaBH_4$ solution (0.1 M in methanol; 30 mL) was added drop-wise, followed by stirring for 10 min. Finally, the suspension was washed with 15 mL each of methanol and H_2O, and then dried in a vacuum concentrator at 50 °C.

2.4. Preparation of DNA probe

Glassy carbon electrodes (GCEs) were treated consecutively with 1.0, 0.3 and 0.05 μm of alumina slurries for 1 min each. The electrodes were washed with water, ethanol, and 1 M HNO_3 before being dried in a nitrogen atmosphere. After cleaning, the surfaces of the GCEs were characterized by recording cyclic voltammetry (CV)

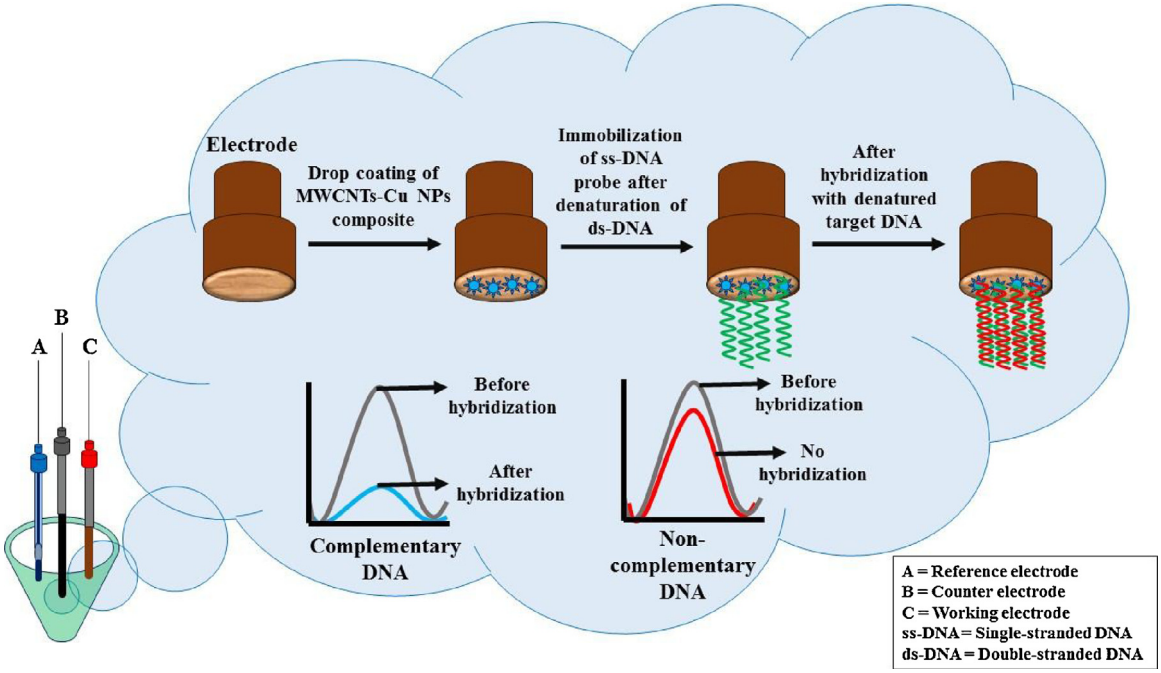

Fig. 1. Schematic diagram illustrating different stages of the development of nano-bio interface based on MWCNTs-Cu NPs composite. The composite was drop coated on GCE surface and then ss-DNA strands were electrostatistically bound to construct a DNA probe.

or differential pulse voltammetry (DPV) scans in a cell containing 15 mL of 50 mM $K_3Fe(CN)_6$ and 1 M KNO_3. For all scans, potential was swept between −1 to 1 V at a scan rate of 100 mVs^{-1} against AgCl as the reference electrode.

Primers were designed to amplify complementary and non-complementary DNA from already available CLCuKoV-Bur (acc. no. AM774294) and GroEL gene (acc. no. AF130421), clones as shown in SI (Fig. S2). MWCNTs-Cu NPs composite (30 mg) was dispersed in 1 mL deionized water. Afterwards, 10 μL of the dispersion was coated on GCE followed by drying at 90 °C for 1 min in an oven. Probe DNA (SI; Section 1.1) was amplified using primer pair CLCV1/CLCV2 from clone of CLCuKoV-Bur (acc. no. AM774294) as a template [20]. The PCR product was denatured at 95 °C and 2 μL DNA was immobilized on the MWCNTs-Cu NPs composite to develop probes. After that, the modified electrode was kept in an oven at 35 °C for 3 h and then immersed in a 0.1% SDS for 10 min to remove unbound probe DNA from the interface. The resulting surface obtained was used as a capture probe for DNA hybridization.

In the present study, DNA probe makes electrostatic binding to copper composite in order to generate functional interface and to support DNA hybridization. Actually, when DNA is adsorbed onto an interface, the strands stick in a potential well. In our case Cu NPs are assumed to act as tiny potential wells and consequently, DNA was unable to diffuse off the surface, but, relatively free to rotate and re-adjusts amply to allow the double helix formation [21]. The design strategy of this interface is shown in Fig. 1.

2.5. Electrochemical measurements

For hybridization, DNA modified biointerface was immersed in 0.01 M PBS containing a specific concentration of target DNA (CLCuKoV-Bur), and then it was rinsed thoroughly with SDS solution to wash the unbound DNA. For studying selectivity, all constituents remained the same except for the incubation of non-complementary DNA (GroEL gene) instead of the complementary target DNA. A three electrode system was used with the modified GCEs as the working electrodes, an Ag/AgCl (3 M KCl) electrode as the reference electrode, and a glassy carbon rod as a counter electrode. Electrochemical measurements were performed in 50 mM $K_3Fe(CN)_6$ in PBS solution (pH = 7.4) and MB (5 mM). CV and DPV techniques were used to determine peak oxidation current changes before and after hybridization. CV experiments were performed by applying the potential in the range of −0.5 to 0.75 V at a scan rate of 100 mVs^{-1} or mentioned otherwise. DPV parameters were as the following: a pulse amplitude of 50 mV, a period of 0.2 s, equilibration (s) time of 60 s and a potential range of −0.5 V and 1.2 V. All electrochemical curves were recorded using the General Purpose Electrochemical System software (GPES version 4.9), whereas data was handled using Microsoft Excel.

2.6. Preparation of samples for microscopic analyses

MWCNTs and MWCNTs-Cu NPs composite, each were dispersed in methanol (1.0 mg/mL). Out of that, 10 μL was used to coat quartz wafers and dried at room temperature. For AFM analysis, a silicon nitride probe (OMCL-TR800PSA-1) with a cantilever of 100 μm thickness having a force constant of 0.57 m^{-1} and resonance frequency of 73 kHz was used for scanning; whereas gold was coated on the detector side of the AFM probe. In the case of SEM, the dispersions of MWCNTs and MWCNTs-Cu NPs composite were dropped onto carbon coated copper grids (200 mesh), respectively.

For both microscopic analyses, three samples of each specimen were prepared and scans/images were taken at a minimum of three different areas to ensure the accuracy of the results.

3. Results and discussion

3.1. Characterization of nanocompsoite

The size, shape, and morphology of MWCNTs and MWCNTs-Cu NPs composite was determined by SEM images in a transmission electron microscope (TEM) mode. Fig. 2A shows the typical morphology of MWCNTs and seamless strands of purified MWCNTs about 20–25 nm can be seen. However, after the formation of the composite the surface morphology of the MWCNTs is changed as the result of the agglomeration of Cu NPs, anchored on the sur-

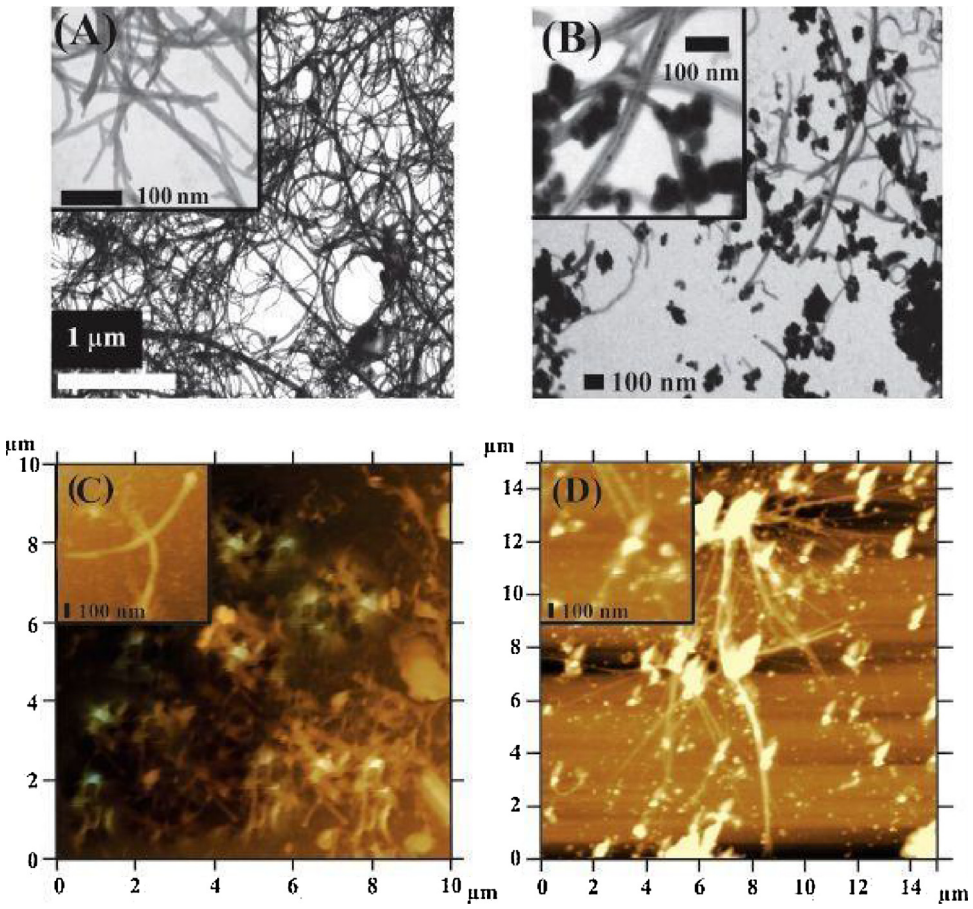

Fig. 2. The FESEM images in TEM mode (A and B) and AFM images (C and D) of MWCNTs and MWCNTs-Cu NPs composite, respectively.

face of MWCNTs (Fig. 2B). These bunches of Cu NPs are irregular in shape possessing rough morphology. Their adhesion indicates strong interactions between Cu NPs and MWCNTs. Furthermore, this interconnected overlapping of MWCNTs, along with the bundles of Cu NPs, ensures a conducting network that can facilitate rapid electron transport during electrode reactions.

MWCNTs and MWCNTs-Cu NPs composites were characterized by AFM (Fig. 2C and D). After surface modification, height of nanotubes was found to be about 50–100 nm, whereas the width of bundles increased *i.e* 20–100 nm, due to agglomeration of Cu NPs (Fig. 2D). NPs were retained and aligned along the whole length of MWCNTs, whereas in different places these existed in the form of patches (about 20–100 nm in height and 20–200 nm in width). Whereas, the diameter of agglomerates was found to be about 100–500 nm (height) and 200–600 nm (width). Comparing SEM and AFM images, it can be observed that AFM evidences are in good agreement with SEM results, thus confirming the presence of Cu NPs on the surface of MWCNTs, as the result of its amine modification.

Surface roughness plays a very important role in fabricating efficient interfaces. Generally, rougher surfaces are assumed to be more active by offering more sites for the binding of analyte, thus contributing to its improved detection. In our case surface roughness could have a direct impact on the sensor signals of the developed bio-interface. The surface roughness parameter, RMS for MWCNTs was calculated to be 7.5 nm, where its value for MWCNTs-Cu NPs composite was found to be 34.35 nm. In a previously developed nsZnO/ITO/DNA biosensor, RMS was found to be only 3.51 nm for the prepared nanomaterials, 50–100 nm in size [22]. Thus, greater surface roughness of the interface prepared in the present study indicates the presence of more number of binding sites and thus better efficiency is expected from this biosensor.

The functionalization of MWCNTs does not involve a physical confinement, but it mainly mediates the surface chemistry for anchoring of other nanostructures in the composite. As MWCNTs are negatively charged, they can offer moieties for electrostatic interaction with other cations. For instance, Pb^{2+}, Cu^{2+} and Cd^{2+} ions can interact with MWCNTs and among them Pb^{2+} and Cu^{2+} have greater affinity as compared to Cd^{2+}. Therefore, we selected Cu^{2+} because of its greater affinity with negatively charged MWCNTs [23] expecting greater synergistic effects, high conductivity, in turn greater sensor sensitivity and selectivity. Negatively charged walls of MWCNTs can absorb a cationic polyelectrolyte like PEI due to electrostatic interactions, where a large number of imine groups in the PEI polymer chain can coordinate with Cu^{2+} ions via their nitrogen atoms. These functional groups are adsorbed on the surface of MWCNTs leading to a very stable colloidal dispersion [24]. With the addition of a reducing agent, copper coordinate complexes can lead to the formation and aggregation of Cu NPs along the whole length of MWCNTs. In support of this hypothesis, we carried out systematic studies of MWCNTs and MWCNTs-Cu NPs composite by observing surface charges (Fig. 3). It can be noted that zeta potential values of MWCNTs and MWCNTs-Cu NPs composite are −18 mV and +30.9 mV, respectively. This change of surface charges along with their magnitude is a strong evidence for the modification of MWCNTs due to the presence of Cu NPs. Certainly, a high amount of positive surface charge is expected to play a pivotal role in the strong binding of DNA with the probe leading to its sensitive detection. Here, NPs act as tiny centers for fast electron transfer rate, whereas their synergistic effects with

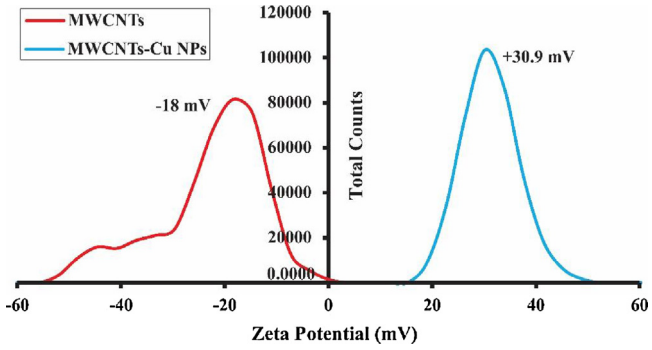

Fig. 3. Plot showing the zeta potentials of MWCNTs (left) and MWCNTs-Cu NPs composite (right) to assess the influence of surface charges on the development of probe interface.

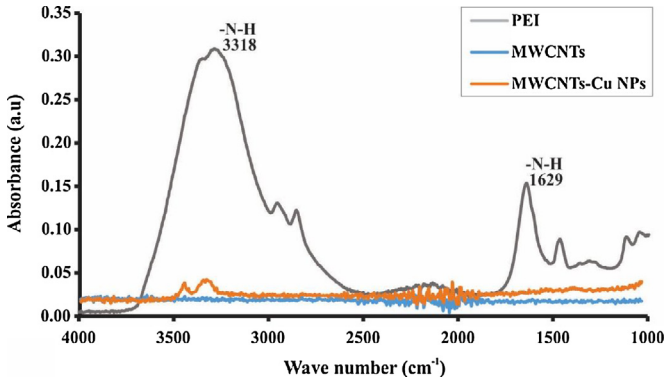

Fig. 4. FT-IR profiles of MWCNTs, MWCNTs-Cu NPs composite and PEI depicting the consumption of the functional moieties in the development of nanocomposite.

MWCNTs and NPs produce differing interactions and higher electrical conductivities, consequently the sensing material offers higher response [25,26]. Furthermore, their morphologies and catalytic properties can be tuned according to application [27]. It is noteworthy that these CNTs nanocomposite can retain metal NPs even if it is washed with nitric acid at high temperatures. Therefore, these can be employed to construct a recognition interface [28]. It has been demonstrated that oligonucleotide probes attached by the simple electrostatic adsorption onto a positively charged surface film produces an extremely stable monolayer of oligonucleotide by this method [21].

Further insight into the mechanism was obtained from FT-IR, a qualitative technique for the evaluation of the functional groups. Fig. 4 illustrates FT-IR spectra of PEI, MWCNTs and MWCNTs-Cu NPs composite, respectively, from 4000 to 1000 cm^{-1}. Noticeable sharp and intensive bands can be seen at 3318 cm^{-1} and 1629 cm^{-1} that arise from the primary and secondary amines (N-H functional groups) of PEI. In the MWCNTs-Cu NPs composite, their intensity is reduced significantly, thus confirming the consumption of these functional groups during the formation of copper complex with PEI, which indirectly validates the formation of MWCNTs-Cu NPs composite.

3.2. Electrochemical investigations of nano-bio interface

It was assumed that by combining charge transport through composite-DNA-modified interfaces to an electrocatalytic cycle involving freely diffusing ferricyanide ions, enhanced selectivity and sensitivity can be achieved. In the present study, for the first time MWCNTs, metal NPs, MB, and ferricyanide are employed as a DNA detection platform. Therefore, foremost of all, it was important to ensure the electrochemical behavior of the composite. The CV responses of $[Fe(CN)_6]^{3-/4-}$ at the bare GCEs and modified electrodes deposited with MWCNTs and the composite, respectively are shown in Fig. 5A. A pair of significant and stable redox peaks appear ($Ip_a = 105 \pm 0.7$ μA and $Ip_c = -150 \pm 0.3$ μA) at the bare GCE (curve a) whereas, these peak currents are much larger for our designed composite (curve c, $Ip_a = 225.6 \pm 0.1$ μA and $Ip_c = -250.3 \pm 0.08$ μA) as compared to bare electrode and MWCNTs. It can be attributed to the synergistic effects of the large specific electrocatalytic surface of Cu NPs and high aspect ratio and electronic conductivity of MWCNTs-Cu NPs composite. This difference in peak currents also validates the electrocatalytic retention of Cu NPs in the prepared composite. Their presence increased the conductivity of the MWCNTs resulting in the increase of the redox peak current (compare curve b and c).

CV technique was further used to evaluate DNA hybridization for the binding of CLCuKoV-Bur with the interface. Fig. 5B displays the CV curves of capture probe in the absence and presence of the target DNA. As the result of immobilization of probe DNA on the surface of MWCNTs-Cu NPs, the redox peak current decreases (Fig. 5B, curve a). After hybridization with target DNA, the redox current even further decreased (Fig. 5B, curve b). It can be ascribed to the formation and presence of double stranded DNA (dsDNA) which greatly inhibited the electron transfer reaction taking place on the interface.

3.3. Basic sensor signals

The hybridization of probe DNA and target DNA was monitored by DPV, which has become the preferred method for investigating the features of functionalized interfaces. As reported previously, functionalized CNTs can bind ssDNA through relatively stable π-stacking interactions [29]. However, in our case charge transfer process is assumed to be strongly affected by the synergistic effects of MWCNTs and Cu NPs and therefore consequent DNA recognition events. For sensitive quantification, DPV were recorded with and without complementary DNA in a background solution, where MB was used as the redox indicator. Therefore, the electrochemical transduction of DNA hybridization is attained using the voltammetric signals of MB at the composite surface. Fig. 6 displays typical DPV scans with 8.1 ng μL^{-1} viral DNA. The highest signal was obtained in case of interface exposed to blank solution. However, when it was immersed in a solution of complementary DNA, the well-defined DPV signal decreased from 7×10^{-4} to 1×10^{-4} amperes (A). This is a strong evidence that interface developed in the present study is capable of responding to the presence of a counterpart DNA strand and thus can be successfully applied to detect virus. This decrease of oxidation current in the presence of MB is similar to other reported work for the detection of DNA specific to *M. tuberculosis* and HBV [22]. Further, it was investigated that this electrode reaction is a diffusion controlled process (SI; Section 1.3) by recording the effect of scan rate on the oxidation peak height (SI; Fig. 3).

3.4. Mechanism of interface interaction

In this method we have used DNA mediated charge transport where positively charged MB binds to the negatively charged ssDNA attached to the composite interface, through attractive coulomb interactions [30]. This increases the concentration of MB near the surface. The electron flows from the interface to reduce MB^+ attached with ssDNA to leucomethylene blue, which in turn reduces solution-produced ferricyanide. As more number of electrons can flow to MB^+, this catalytic cycle continues to generate current and the interface-bound DNA is continually investigated. The highest MB reduction signal was observed with the ssDNA probe, immobilization onto the MWCNTs-Cu NPs-modified sur-

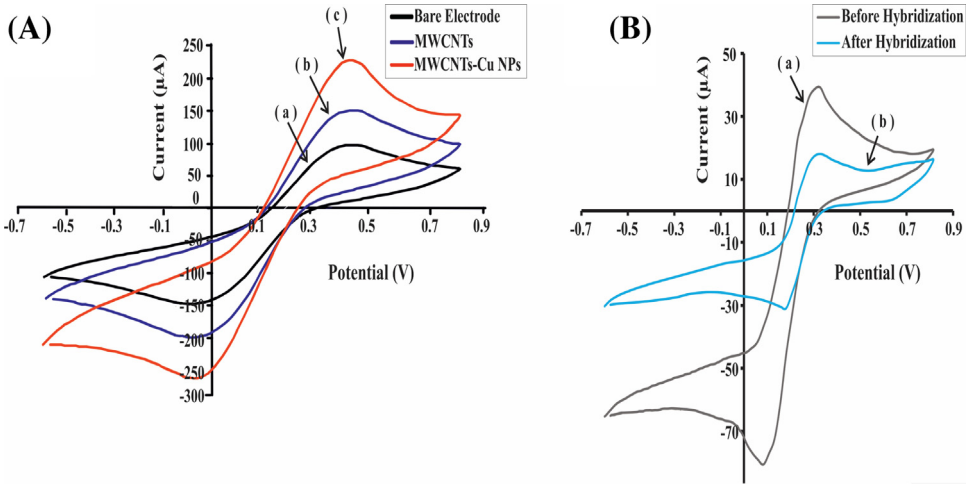

Fig. 5. The electrochemical performance of interfaces (A) CV signals of bare (a) MWCNTs (b) and MWCNTs-Cu NPs (c) interfaces in 50 mM $[Fe(CN)_6]^{3-/4-}$ and PBS (pH = 7.4); (B) CV responses of MWCNTs-Cu NPs-probe interface in blank solution (a) and with respect to complementary DNA (CLCuKoV-Bur, 8.1 ng μL^{-1}) (b), $[Fe(CN)_6]^{3-/4-}$ (50 mM), methylene blue (5 mM), PBS (pH = 7.4), scan rate 100 mVs^{-1}. (For interpretation of the references to colour in this figure legend, the reader is referred to the web version of this article.)

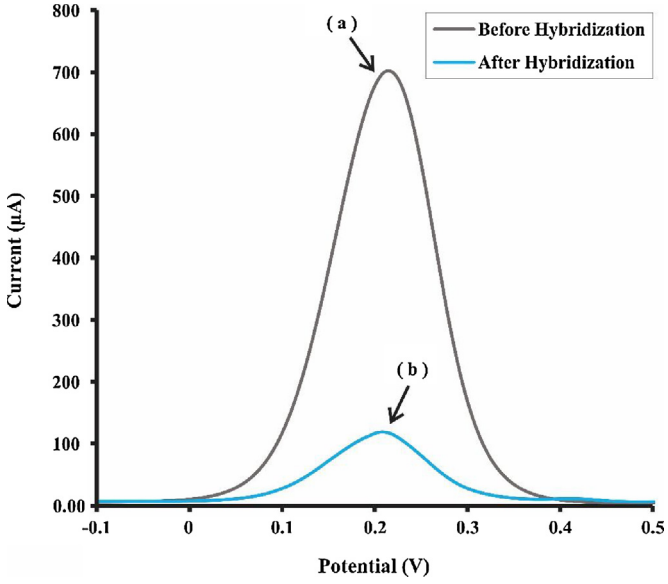

Fig. 6. DPV profiles of MWCNTs-Cu NPs-probe interface in background solution and with complementary DNA strands (CLCuKoV-Bur; 8.1 ng μL^{-1}); $[Fe(CN)_6]^{3-/4-}$ (50 mM), methylene blue (5 mM), PBS (pH = 7.4), scan rate 100 mVs^{-1}. (For interpretation of the references to colour in this figure legend, the reader is referred to the web version of this article.)

face alone (Fig. 6, curve a), because the greatest amount of MB accumulation occurs at the electrode surface in that case. On the other hand, when the sequences of the target and the probe are complementary, they hybridize to form dsDNA. In double-stranded duplexes the bases are arranged in a helical structure and the concentration of MB near the interface decreases due to the absence of MB attached to ssDNA. An obvious decrease in the voltammetric peak was observed as the indicator after duplex formation (Fig. 6, curve b), because the electrocatalytic cycle of MB was prevented by hybrid formation on the electrode surface. Thus the lowest MB reduction signal was obtained from the full hybrid with the target DNA sequence on the electrode surface. In essence, it can be said, the concentration of MB near the interface is higher for non-complementary targets and probes than for complementary ones [31]. As this kind of assay is not a measure of differential hybridization, mismatches, can be detected without stringent hybridization conditions and the interface can be used for the facile and sensitive DNA detection [32].

3.5. Analytical parameters

The analytical performance of the designed biosensor was investigated and Fig. 7 shows DPV scans after hybridization with different target DNA concentrations (1×10^{-10} to 1×10^{-14} g μL^{-1}) using MWCNTs-Cu NPs-probe modified GCEs. The decrease in oxidation current signals was found inversely proportional to increasing target DNA concentrations. The sensor response was found linearly dependent upon the log of target DNA concentration with $R^2 = 0.9932$ (Inset Fig. 7). The detection limit (LOD), taken as the concentration that gives a signal equal to three times the standard deviation of the blank signal, was found to be 0.01 ng μL^{-1} (n = 6, S/N = 3). Whereas, limit of quantification (LOQ) were found to be 0.04 ng μL^{-1} (n = 6, S/N = 10). We compared the detection limit of our proposed sensor with other published methods and data has been summarized in Table 1. As can be seen from the data, the DNA biosensor developed in the present study shows a high sensitivity as compared to the other forms of nanomaterials, composite, and interfaces. This implies that the designed interface can be used to detect DNA presence for diseases where infection level is low enough to show symptoms. Thus we have developed a nano/bio interface by a facile and straightforward method with similar sensitivity for the detection of viral DNA without performing laborious laboratory techniques like real-time quantitative PCR (qPCR).

3.6. Reproducibility and stability

A series of ten modified interfaces was prepared and exposed to target DNA solutions (8.1 ng μL^{-1}). Each individual oxidation current value was calculated as the average of fifty DPV scans. Fig. 8A depicts the outcome of this experiment which shows the prepared biosensor is stable, as can be seen from the comparably small error bars (The relative standard deviation was found to be 1.37). The same is true for the reproducibility if we calculate the average of the first and the last two cycles, respectively (698.5 ± 1 μA and 697.5 ± 2 μA) and compare them, the total loss of signal is only 0.28% of the original oxidation current value (700 ± 0.9 μA). It can be concluded that unlike conventional methods, another merit of this sensing platform is that the probe can be reused. Thus, on the one hand it is a sensitive and on the other hand a very cheap

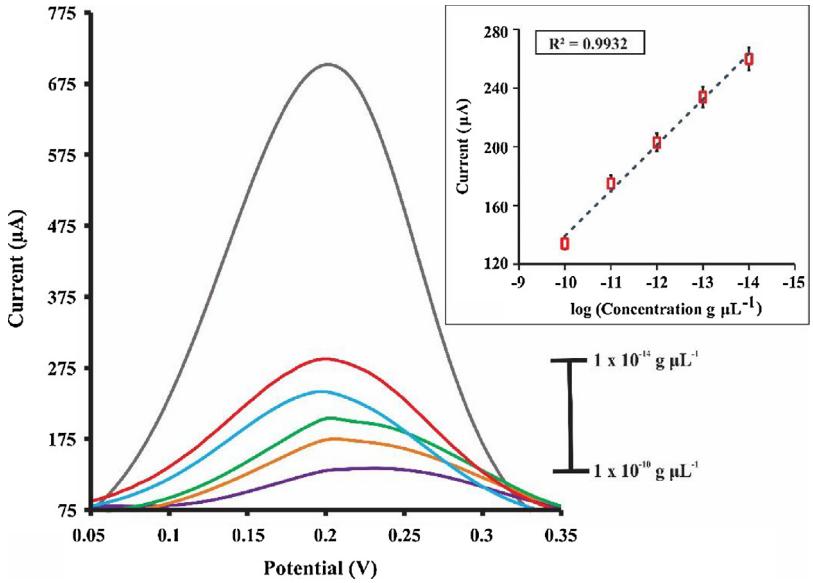

Fig. 7. Analytical performance of the nano-bio interface; DPV profiles of MWCNTs-Cu NPs-probe modified GCE before and after hybridization with complementary DNA (CLCuKoV-Bur) from 1×10^{-10} to 1×10^{-14} g µL^{-1}; $[Fe(CN)_6]^{3-/4-}$ (50 mM), methylene blue (5 mM), PBS (pH = 7.4), scan rate 100 mVs^{-1}; Inset showing linearity of the sensor responses with respect to different target DNA concentrations. (For interpretation of the references to colour in this figure legend, the reader is referred to the web version of this article.)

Table 1
Comparison of the analytical parameters of present nano-bio interface with other reported materials for DNA detection.

Materials	Techniques	Target DNA	Sensitivity (ng µL^{-1})	Reference
Biosensor based on gold nanoparticles for tuberculosis detection	DPV	*Mycobacterium tuberculosis*	0.05	[33]
Flower-like zinc oxide nanostructure based electrochemical DNA biosensor	DPV	Meningitis	5	[34]
Zirconium oxide (ZrO_2) film deposited on to the gold surface	DPV	*Mycobacterium tuberculosis*	0.065	[35]
DNA sensor based on thiol modified hemi-methylated hairpin probe DNA	DPV	Demethylated DNA	170	[36]
Electrochemical DNA biosensor based on gold nanoleaves	DPV	*Leishmania major*	0.07	[37]
Methylene Blue, PGE, 20- mer single strand oligonucleotide probe related to human papilloma virus (HPV) major capsid protein L1 gene	SWV	*Human papillomavirus*	1.2	[38]
Electrochemical biosensor based on gold particles and DNA probe	DPV	Demethylated DNA caused by endonuclease BstUI and exonuclease III digestions	150	[39]
Nickel doped zinc oxide thin film based sensitive DNA biosensor	DPV	Meningitis	5	[40]
Multi-walled carbon nanotubes-copper nanoparticles (MWCNTs-Cu NPs) composite and CLCuKoV-Bur DNA deposited on glassy carbon electrode	DPV	*Cotton leaf curl Khokhran virus*-Burewala (CLCuKoV-Bur)	0.01	This work

DPV: Differential Pulse Voltammetry.
SWV: Square Wave Voltammetry.

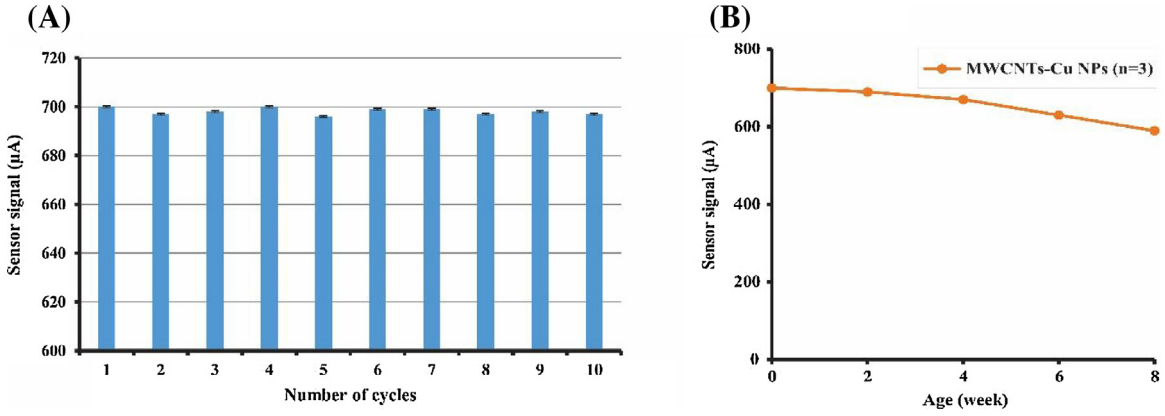

Fig. 8. The sensor characteristics (A) reproducibility of sensor signals towards target DNA (CLCuKoV-Bur; 8.1 ng µL^{-1}) (B) effect of aging on the MWCNTs-Cu NPs-probe interface. The responses were measured once every two weeks towards target DNA (CLCuKoV-Bur; 8.1 ng µL^{-1}).

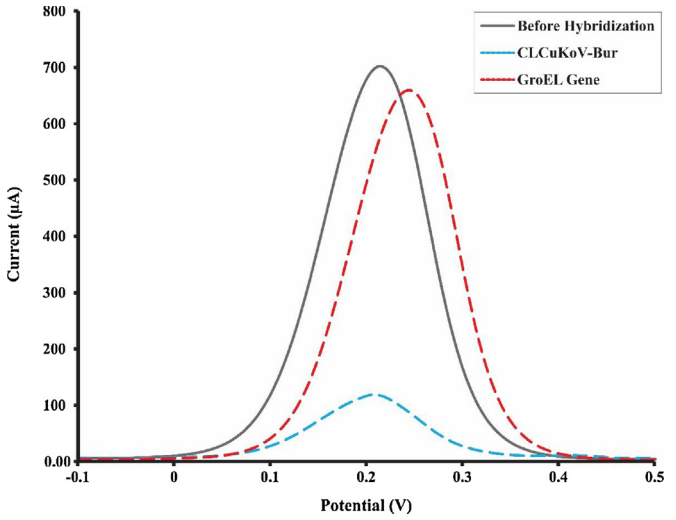

Fig. 9. DPV signals of MWCNTs-Cu NPs-probe interface before and after incubation with complementary DNA (CLCuKoV-Bur; 8.1 ng μL^{-1}) and non-complementary DNA (GroEL gene; 8.5 ng μL^{-1}); $[Fe(CN)_6]^{3-/4-}$ (50 mM), methylene blue (5 mM), PBS (pH = 7.4), scan rate 100 mVs^{-1}. (For interpretation of the references to colour in this figure legend, the reader is referred to the web version of this article.)

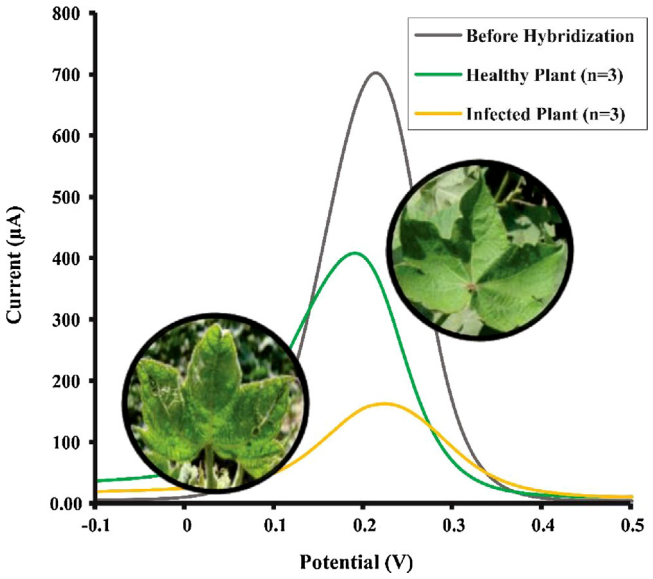

Fig. 10. DPV signals of MWCNTs-Cu NPs-probe interface in background solution alone and with leaf sap of healthy and infected plants; $[Fe(CN)_6]^{3-/4-}$ (50 mM), methylene blue (5 mM), PBS (pH = 7.4), scan rate 100 mVs^{-1}. (For interpretation of the references to colour in this figure legend, the reader is referred to the web version of this article.)

method in the long run. To evaluate ruggedness, we studied aging effects of the constructed interfaces by exposing them to target DNA (8.1 ng μL^{-1}) during defined periods of time. The results are shown in Fig. 8B. For these experiments, the modified GCEs were kept at 4 °C in phosphate buffered saline (PBS) solution, when not in use. It can be seen in that biosensor responded in a stable manner for four weeks as it lost only 4.3% of the initial oxidation current value of a freshly prepared electrode. However, after eight weeks a considerable loss of current was observed, calculating 15%. One reason for this may be oxidation of the composite material with the passage of time.

3.7. Selectivity studies

The specificity of the DNA biosensor was investigated by incubating it with complementary and non-complementary DNA sequences. Fig. 9 shows the DPV signals before and after hybridization with the same amount of target DNA (CLCuKoV-Bur; 8.1 ng μL^{-1}) and non-complementary DNA (GroEL gene; 8.1 ng μL^{-1}). The highest signal was obtained using the DNA probe alone, whereas a large decrease in the signal was observed in the presence of the target sequence. The sensor shows 97.14% selectivity as a great DPV peak was observed when the probe was exposed to GroEL gene DNA. This indicates that there was no hybridization between the probe and the non-specific DNA, in turn a good electrochemical performance of the prepared composite. These findings strongly demonstrated that DNA biosensor using MWCNTs-Cu NPs composite showed highly efficient and selective detection towards CLCuKoV-Bur DNA.

3.8. Detection of CLCuKoV-Bur DNA in infected plant leaves

In this study, we have taken a step forward towards the real application of nanomaterials based bio-interfaces, for detection of virus infection in field infected cotton plants. Leaves of cotton plants with CLCuD symptoms were collected from three different areas of a cotton field. Leaf tissue (100 mg) was ground to a fine powder in a sterile pestle mortar, adding about 1 mL deionized water. Then 15 μL of resultant leaf sap was exposed to the DNA probe. Each individual sensor signal is an average of three freshly prepared electrodes and fifty scans of each. Fig. 10 shows representative DPV curves. A significant difference between very well defined oxidation current signals of sap extracted from healthy and infected plants is evident, showing the presence of CLCuKoV-Bur virus in the leaf samples. It also implies that the developed interface exhibit high accuracy and sensitivity for the detection of virus in cotton plants. Undoubtedly, further optimization of this method is required, such as using different sap isolation methods to remove impurities or direct DNA extraction that may improve sensitivity further. Nonetheless, this method can be used as a tool for the early identification of plant viruses, especially when physical symptoms are not apparent. These results further indicate that similar types of nano-bio interfaces can be constructed with different versatility, for the detection of other pathogens or bio-organism based on their unique DNA sequences.

4. Conclusions

The reported nanocomposite based probe in this study demonstrates a highly sensitive and selective method for detection of cotton plant virus. For the first time, MWCNTs, metal NPs, MB, and ferricyanide are tailored together to construct a recognition layer where MWCNTs-Cu NPs composite is used for the immobilization of a probe DNA. SEM and AFM showed that in the prepared composite, Cu NPs (20–100 nm) are retained and aligned along the lengths of MWCNTs, thus offering more number of binding positions for the development of the nano-bio probe. Surface potential values support the presence of positive change on the prepared composite for the attachment of viral DNA. The detection of hybridization was accomplished using the reduction signals of MB, where the electroactivity of this molecule allows the discrimination of the hybrid surface from the probe facade. The decrease in the magnitude of the reduction signals of MB thus reflected the extent of hybrid formation. It should be noted that electrochemical signals exhibit good characteristics, such as a robust response, sensitivity, and selectivity in comparison to the conventional techniques. This interface was proved successful for the detection of virus in field-collected cotton leaves samples. This nano-bio platform will be suitable for detecting other viruses, particularly when symptoms are not apparent by naked eyes.

Competing interests

The authors declare no competing financial interest.

Acknowledgements

This material is based upon work supported by the "Pak-US cotton productivity enhancement program" of the International Center for Agricultural Research in the Dry Areas (ICARDA) funded by the United States Department of Agriculture (USDA), Agricultural Research Service (ARS), under agreement No. 58-6402-0-178F. Any opinions, findings, conclusions or recommendations expressed in this publication are those of the author(s) and do not necessarily reflect the views of the USDA or ICARDA. This research work is also partially supported by the International Foundation for Science (IFS) Sweden by a Research Grant no. E-5659. Authors are thankful to Mr. Muhammad Bilal Haider for providing clone of GroEL gene.

Appendix A. Supplementary data

Supplementary data associated with this article can be found, in the online version, at https://doi.org/10.1016/j.jhazmat.2017.12.007.

References

[1] L. Yang, Y. Tao, G. Yue, R. Li, B. Qiu, L. Guo, Z. Lin, H.-H. Yang, Highly selective and sensitive electrochemiluminescence biosensor for p53 DNA sequence based on nicking endonuclease assisted target recycling and hyperbranched rolling circle amplification, Anal. Chem. 88 (2016) 5097–5103.
[2] H.Y. Lau, H. Wu, E.J. Wee, M. Trau, Y. Wang, J.R. Botella, Specific and sensitive isothermal electrochemical biosensor for plant pathogen DNA detection with colloidal gold nanoparticles as probes, Sci. Rep. 7 (2017) 38896.
[3] K.B. Mullis, F.A. Faloona, Specific synthesis of DNA in vitro via a polymerase-catalyzed chain reaction, Methods Enzymol. 155 (1987) 335–350.
[4] E.M. Southern, Detection of specific sequences among DNA fragments separated by gel electrophoresis, J. Mol. Biol. 98 (1975) 503–517.
[5] K.J. Angelis, M. Dusinska, A.R. Collins, Single cell gel electrophoresis: detection of DNA damage at different levels of sensitivity, Electrophoresis 20 (1999) 2133–2138.
[6] M. Khan, A.R. Khan, J.-H. Shin, S.-Y. Park, A liquid-crystal-based DNA biosensor for pathogen detection, Sci. Rep. 6 (2016) 22676.
[7] J. Ping, R. Vishnubhotla, A. Vrudhula, A.C. Johnson, Scalable production of high-sensitivity, label-free DNA biosensors based on back-gated graphene field effect transistors, ACS Nano 10 (2016) 8700–8704.
[8] S. Wang, L. Zhang, S. Wan, S. Cansiz, C. Cui, Y. Liu, R. Cai, C. Hong, I.-T. Teng, M. Shi, Aptasensor with expanded nucleotide using DNA nanotetrahedra for electrochemical detection of cancerous exosomes, ACS Nano 11 (2017) 3943–3949.
[9] Q. Zhao, Y. Zhou, Y. Li, W. Gu, Q. Zhang, J. Liu, Luminescent iridium (III) complex labeled DNA for graphene oxide-based biosensors, Anal. Chem. 88 (2016) 1892–1899.
[10] C. Zhao, F. Gao, S. Weng, Q. Liu, L. Lin, X. Lin, An electrochemical sensor based on DNA polymerase and HRP-SiO 2 nanoparticles for the ultrasensitive detection of K-ras gene point mutation, RSC Adv. 6 (2016) 8669–8676.
[11] M. Chehelamirani, M.C. da Silva, D.R. Salahub, Electronic properties of carbon nanotubes complexed with a DNA nucleotide, Phys. Chem. 19 (2017) 7333–7342.
[12] N. Karousis, I. Suarez-Martinez, C.P. Ewels, N. Tagmatarchis, Structure, properties, functionalization, and applications of carbon nanohorns, Chem. Rev. 116 (2016) 4850–4883.
[13] C.J. Serpell, K. Kostarelos, B.G. Davis, Can carbon nanotubes deliver on their promise in biology? Harnessing unique properties for unparalleled applications, ACS Cent. Sci. 2 (2016) 190–200.
[14] M.R. Ojaghian, J.-Z. Zhang, F. Zhang, W. Qiu, X.-L. Li, G.-L. Xie, S.-J. Zhu, Early detection of white mold caused by Sclerotinia sclerotiorum in potato fields using real-time PCR, Mycol. Prog. 15 (2016) 959–965.
[15] J.K. Brown, F.M. Zerbini, J. Navas-Castillo, E. Moriones, R. Ramos-Sobrinho, J.C.F. Silva, E. Fiallo-Olivé, R.W. Briddon, C. Hernández-Zepeda, A. Idris, V.G. Malathi, D.P. Martin, R. Rivera-Bustamante, S. Ueda, A. Varsani, Revision of Begomovirus taxonomy based on pairwise sequence comparisons, Arch. Virol. 160 (2015) 1593–1619.
[16] F.M. Zerbini, R.W. Briddon, A. Idris, D.P. Martin, E. Moriones, J. Navas-Castillo, R. Rivera-Bustamante, P. Roumagnac, A. Varsani, ICTV virus taxonomy profile: geminiviridae, J. Gen. Virol. 98 (2017) 131–133.
[17] S.S.-e.-A. Zaidi, M. Shafiq, I. Amin, B.E. Scheffler, J.A. Scheffler, R.W. Briddon, S. Mansoor, Frequent occurrence of Tomato leaf curl New Delhi virus in cotton leaf curl disease affected cotton in Pakistan, PLoS One 11 (2016) e0155520.
[18] S. Takalkar, K. Baryeh, G. Liu, Fluorescent carbon nanoparticle-based lateral flow biosensor for ultrasensitive detection of DNA, Biosens. Bioelectron. 98 (2017) 147–154.
[19] M. Jin, X. Liu, A. van den Berg, G. Zhou, L. Shui, Ultrasensitive DNA detection based on two-step quantitative amplification on magnetic nanoparticles, Nanotechnology 27 (2016), 335102.
[20] S. Akhtar, R.W. Briddon, S. Mansoor, Reactions of Nicotiana species to inoculation with monopartite and bipartite begomoviruses, Virol. J. 8 (2011) 475.
[21] C. Altay, R.H. Senay, E. Eksin, G. Congur, A. Erdem, S. Akgol, Development of amino functionalized carbon coated magnetic nanoparticles and their application to electrochemical detection of hybridization of nucleic acids, Talanta 164 (2017) 175–182.
[22] M. Das, G. Sumana, R. Nagarajan, B.D. Malhotra, Application of nanostructured ZnO films for electrochemical DNA biosensor, Thin Solid Films 519 (2010) 1196–1201.
[23] A. Munawar, M.A. Tahir, A. Shaheen, P.A. Lieberzeit, W.S. Khan, S.Z. Bajwa, Investigating nanohybrid material based on 3D CNTs@Cu nanoparticle composite and imprinted polymer for highly selective detection of chloramphenicol, J. Hazard. Mater. 342 (2018) 96–106.
[24] J. Yu, N. Grossiord, C.E. Koning, J. Loos, Controlling the dispersion of multi-wall carbon nanotubes in aqueous surfactant solution, Carbon 45 (2007) 618–623.
[25] H. Wang, S. Li, Y. Si, Z. Sun, S. Li, Y. Lin, Recyclable enzyme mimic of cubic Fe3O4 nanoparticles loaded on graphene oxide-dispersed carbon nanotubes with enhanced peroxidase-like catalysis and electrocatalysis, J. Mater. Chem. B 2 (2014) 4442–4448.
[26] H. Wang, S. Li, Y. Si, N. Zhang, Z. Sun, H. Wu, Y. Lin, Platinum nanocatalysts loaded on graphene oxide-dispersed carbon nanotubes with greatly enhanced peroxidase-like catalysis and electrocatalysis activities, Nanoscale 6 (2014) 8107–8116.
[27] D. Gioia, I.G. Casella, Pulsed electrodeposition of palladium nano-particles on coated multi-walled carbon nanotubes/nafion composite substrates: electrocatalytic oxidation of hydrazine and propranolol in acid conditions, Sens. Actuator B-Chem. 237 (2016) 400–407.
[28] M. Pumera, Carbon nanotubes contain residual metal catalyst nanoparticles even after washing with nitric acid at elevated temperature because these metal nanoparticles are sheathed by several graphene sheets, Langmuir 23 (2007) 6453–6458.
[29] J. Li, E.-C. Lee, Functionalized multi-wall carbon nanotubes as an efficient additive for electrochemical DNA sensor, Sens. Actuator B-Chem. 239 (2017) 652–659.
[30] C.-Y. Lee, K.-Y. Wu, H.-L. Su, H.-Y. Hung, Y.-Z. Hsieh, Sensitive label-free electrochemical analysis of human IgE using an aptasensor with cDNA amplification, Biosens. Bioelectron. 39 (2013) 133–138.
[31] J. Li, E.-C. Lee, Carbon nanotube/polymer composite electrodes for flexible, attachable electrochemical DNA sensors, Biosens. Bioelectron. 71 (2015) 414–419.
[32] L. Wu, H. Ji, H. Sun, C. Ding, J. Ren, X. Qu, Label-free ratiometric electrochemical detection of the mutated apolipoprotein E gene associated with Alzheimer's disease, Chem. Commun. 52 (2016) 12080–12083.
[33] S.R. Torati, V. Reddy, S.S. Yoon, C. Kim, Electrochemical biosensor for Mycobacterium tuberculosis DNA detection based on gold nanotubes array electrode platform, Biosens. Bioelectron. 78 (2016) 483–488.
[34] M. Tak, V. Gupta, M. Tomar, Flower-like ZnO nanostructure based electrochemical DNA biosensor for bacterial meningitis detection, Biosens. Bioelectron. 59 (2014) 200–207.
[35] M. Das, G. Sumana, R. Nagarajan, B.D. Malhotra, Zirconia based nucleic acid sensor for Mycobacterium tuberculosis detection, Appl. Phys. Lett. 96 (2010) 133703.
[36] Q. Shen, M. Fan, Y. Yang, H. Zhang, Electrochemical DNA sensor-based strategy for sensitive detection of DNA demethylation and DNA demethylase activity, Anal. Chim. Acta 934 (2016) 66–71.
[37] M. Moradi, N. Sattarahmady, A. Rahi, G.R. Hatam, S.M.R. Sorkhabadi, H. Heli, A label-free, PCR-free and signal-on electrochemical DNA biosensor for Leishmania major based on gold nanoleaves, Talanta 161 (2016) 48–53.
[38] R.E. Sabzi, B. Sehatnia, M.H. Pournaghi-Azar, M.S. Hejazi, Electrochemical detection of human papilloma virus (HPV) target DNA using MB on pencil graphite electrode, JICS 5 (2008) 476–483.
[39] H. Yin, Z. Yang, B. Li, Y. Zhou, S. Ai, Electrochemical biosensor for DNA demethylase detection based on demethylation triggered endonuclease BstUI and Exonuclease III digestion, Biosens. Bioelectron. 66 (2015) 266–270.
[40] M. Tak, V. Gupta, M. Tomar, An electrochemical DNA biosensor based on Ni doped ZnO thin film for meningitis detection, J. Electroanal. Chem. 792 (2017) 8–14.